Fusion Engineering and Design 150 (2020) 111369

Contents lists available at ScienceDirect

Fusion Engineering and Design

journal homepage: www.elsevier.com/locate/fusengdes

An improved substructuring approach for dynamic modelling – The example of the ITER vacuum vessel

Fabrizio Di Martino[a,*], Tyge Schioler[b], Giulio Sannazzaro[b], Donato Aquaro[a], Rosa Lo Frano[a]

[a] University of Pisa, Civil and Industrial Engineering Department, Largo Lucio Lazzarino 2, 56126, Pisa, Italy
[b] ITER Organization, Route de Vinon-sur-Verdon, CS 90 064, 13067 St. Paul Lez Durance Cedex, France

ARTICLE INFO

Keywords:
ITER
Vacuum vessel
Seismic
Finite element
Substructuring

ABSTRACT

This study deals with the substructuring method that is adopted for treating complex structures, such as the ITER Tokamak, as an assembly of different components or substructures. This method uses basic mass and stiffness matrices combined with conditions representative of the geometrical compatibility along the substructure boundaries. This approach makes it possible to simulate the dynamic behaviour of the (complex) ITER Vacuum Vessel (VV), subjected to dynamic loading (e.g. seismic), by means of a simplified model (finite element discretization) with little loss of accuracy. In this framework, a simplified model of the ITER VV for use in global seismic analyses has been developed and implemented. In order to minimize the wavefront (and hence computational time), the simplified model is made of multiple superelements, each representing a part of the VV. Moreover, in order to reduce the number of Degrees of Freedom (DoFs) needed along the boundaries of the different substructures, a new approach has also been developed for the breakdown of the benchmark model.

1. Introduction

Understanding of the dynamic response of the Tokamak machine and its components due to a seismic event is important to ensure that its design is compliant with safety requirements for seismic loads.

From a dynamic point of view, the ITER machine sits inside a building that is horizontally isolated from the ground (Fig. 1). The vertical modes of the two main components of the machine (the VV and the magnet system) interact dynamically with each other and with the building. To capture such interaction, without introducing excessive conservatism, it is useful to represent all the significant systems of the Tokamak machine (e.g. Magnets, Cryostat, Vacuum Vessel, etc.) in one analysis. In doing that, each component has to be represented with its mass and stiffness and related uncertainties. In order for the analyses to run in a reasonable time, it is useful to use simplified models. Such simplified models should be capable of simulating the behaviour of the detailed benchmark models without losing accuracy.

Although several methodologies exist for creating such simplified models, such as those summarized in [1–3], in this study the substructuring approach is used. This method allows to perform accurate dynamic analysis and to reduce the computational cost. The substructuring approach makes use of the Guyan reduction method [4–6], which condensates the system matrices on a smaller number of DoFs. The Guyan reduction therefore allows the size of each substructure (finite element models) to be reduced.

The modelling approach is validated using criteria based on the ability of the resulting model to reproduce the behaviour of the benchmark model. A detailed model of the VV is used as input for the substructuring analysis of the Vacuum Vessel. The VV model has to be used in dynamic calculations together with other simplified models to form the whole ITER Tokamak Machine, so in this sense the lightness of the model is important.

In the following Section 2 the substructuring approach based on the Guyan reduction method is described. Section 3 provides the validation of the simplified model of the VV. Results obtained from the application of this method are presented and discussed.

2. Substructuring method

2.1. Methodology description

The substructuring method is based on the Guyan reduction method, which condensates the system matrices on a smaller number of degrees of freedom [4,6], hereafter called master DoFs. Indeed, the accuracy depends on the a-priori selection of these master DoFs.

In the substructuring method [7], the structure is partitioned into a number of substructures. It is important to note that the partition greatly affects the matrix formulation, so the partitioning must be done

* Corresponding author.
E-mail address: f.dimartino2@studenti.unipi.it (F. Di Martino).

https://doi.org/10.1016/j.fusengdes.2019.111369
Received 31 May 2019; Received in revised form 18 September 2019; Accepted 14 October 2019
Available online 02 November 2019

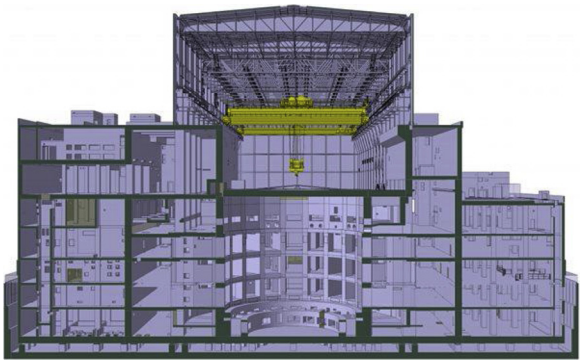

Fig. 1. Scheme of the Tokamak Complex.

carefully. Once substructures have been created, they are assembled by coupling coincident nodes on the boundaries.

The VV structure is divided into substructures based on the geometry or modelling convenience. Each substructure is analysed separately in order to reduce the system matrices to a smaller set of DoFs. The resultant of the substructure method is a so-called superelement [5], which groups elements meeting certain conditions (defined mathematically) and that, upon assembly, may be regarded as an individual structural element for computational purposes. This superelement can be used directly in an analysis or can be used to create more superelements (multi-level substructure).

2.2. Partition interface

When the partition of the model is performed, all the DoFs, both displacements and rotations, on the interface of the substructure must be selected as master DoFs. For models like the ITER VV, that implies that for each subcomponent, a huge number of DoFs should be selected. This causes a substantial increase of the wavefront value, i. e. the maximum number of non-zero entries in a row of the stiffness matrix.

In this paper a method is presented to reduce the number of DoFs on the boundary, without losing confidence on the good behaviour of the structure. This method has been developed for shell elements using the ANSYS Mechanical APDL code. More studies must to be carried out to extend the application of the method to other element types. In the following paragraphs, a brief description of some used commands or nomenclatures of the code is provided.

Fig. 2 left shows a sketch of an initial shell mesh of a structure while Fig. 2 right shows the same mesh after being divided into two parts. The red dots represent the selected master nodes DoFs. These DoFs will be rigidly linked by means of coupling (CP). In this case, not all of the nodes on the interface are chosen as master nodes.

If "few" master DoFs are selected at the boundary, the interface stiffness is underestimated. This selection will produce a detachment of the mesh where the nodes are not directly connected, as shown in Fig. 3.

To avoid this problem, the average motion of all the interface nodes must be considered. To achieve this, all nodes on the interface, hereafter called slave nodes, are connected through RBE3 links [8] to the nearest selected master node, as shown in Fig. 4.

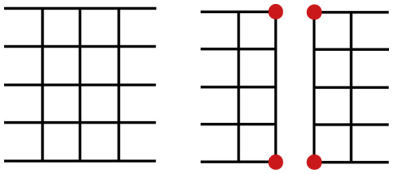

Fig. 2. Initial mesh (left). Division of the mesh with the master DoFs selected (right).

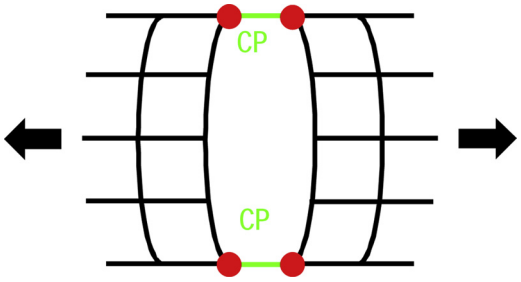

Fig. 3. Effect of the selection of few DoFs on the interface.

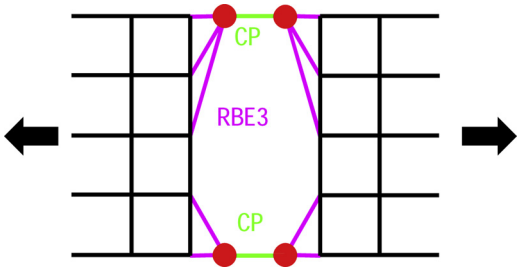

Fig. 4. Interface connection: the RBE3 is represented through the magenta link, while the CP are in green.

If a set of slave nodes for a given RBE3 are collinear, the potential for drilling must be taken into account. In this case, drilling refers to the fact that the master node rotation parallel to the collinear direction cannot be determined in terms of translations of the slave nodes. The moment about the collinear axis therefore cannot be transmitted, and the RBE3 cannot be defined.

To solve this problem, for each element attached to each slave node, two more nodes are created. These are placed normal to the element surface, at the extremes of the element thickness. For this reason they are hereafter referred to as "external" nodes. These nodes are rigidly linked to the relevant slave node through Constraint Equations (CEs), and to the master node by means of RBE3. Moreover weighting factors (WFs) are applied to take into account the area of influence of each slave node.

For each RBE3 the vector of WFs is defined as:

$$\{WF\} = \{WF_1,\ WF_2,\ \ldots, WF_k,\ \ldots, WF_n\} \tag{1}$$

With reference to Fig. 5, the WF for each external node is:

$$WF_k = \frac{A_k}{A_{tot}} \tag{2}$$

Where: A_{tot} is the total area of the elements at the interface, given as:

$$A_{tot} = L_{tot} \bullet t \tag{3}$$

A_k is the influence area of the node k:

$$A_k = \frac{L_{elm}}{2} \bullet \frac{t}{2} = \frac{L_{elm} \bullet t}{4} = \frac{A_{elm,k}}{4} \tag{4}$$

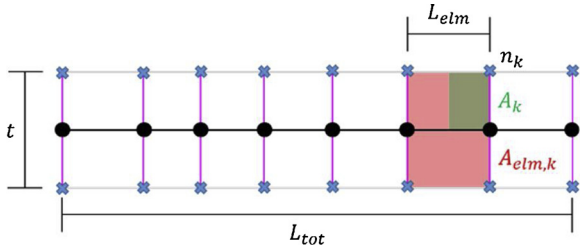

Fig. 5. Geometrical parameters used for WFs calculation. A_k is the green rectangle, $A_{elm,k}$ is the red rectangle (where ¼ is covered by the green one).

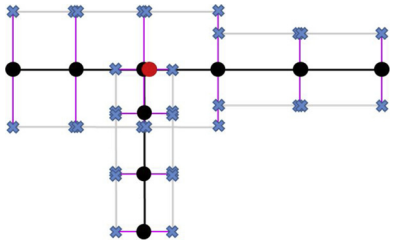

Fig. 6. Layout of the external nodes in case of different thickness and orientation of adjacent elements. The external nodes are the blue crosses. The master node is the red dot.

L_{tot} is the total length of the elements considered in the connection;
t is the thickness of the element;
L_{elm} is the length of the single element.
$A_{elm,k}$ is the area of the single element.

As stated before, for each slave node two external nodes are created for each element that contains the node. Fig. 6 shows that for each slave node, two external nodes are created. The reason for creating a number of external nodes proportional to the elements attached to the slave node is to take into account discontinuities in thickness, or different orientations of two adjacent elements.

Because the matrix condensation cannot be performed on nodes that belong to CEs, the master node of the RBE3 connection is duplicated and the two nodes are linked with very stiff spring (COMBIN14) elements. The final layout of the interface is shown in Fig. 7.

2.3. Benchmark model breakdown and simplified model creation

The simplified model is obtained by performing substructuring analysis on the benchmark model [1]. The benchmark model is partitioned in multiple components, as follow (Fig. 8):

- 9 Sectors of Inboard VV body (in pink);
- 9 Sectors of Outboard VV body with the lower port structure (in grey);
- 18 Upper Ports (in cyan);
- 14 Equatorial Ports (in blue);
- 3 Neutral Beam Ports (HNB1 + DNB in red, HNB2 in yellow and HNB3 in magenta);
- 1 Divertors, corresponding to 54 divertor cassettes (in green only 1/9 of the partitioned component).

The blanket modules are also represented in the model by means of their masses directly condensed on the master nodes selected in the main VV body.

For the Vacuum Vessel Gravity Supports (VVGS) and the port plugs (PP), the elements defined in the benchmark model are directly used in the simplified model (Fig. 9).

Finally, for visualization purposes, dummy elements (solid and shell type) with no mass or stiffness are created. Fig. 9 shows the overview of the simplified model of the VV.

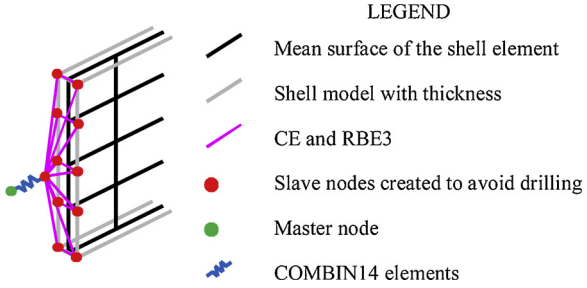

Fig. 7. Layout of the interface connection.

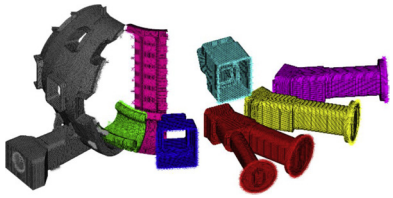

Fig. 8. Partition of the detailed model.

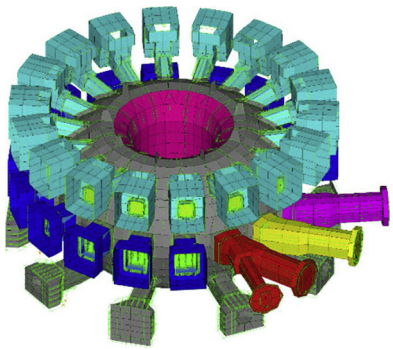

Fig. 9. Simplified model of the Vacuum Vessel.

2.4. Damping ratio and non-linearity

The damping of the superelements is considered in a similar manner to that of traditional elements. A constant damping ratio of 4% is defined for the whole VV system for a Category IV earthquake [9]. The effect of damping on the solved eigenmodes is strictly dependent on the solver used in the modal analysis. Considering the relatively low damping, the Block Lanczos solver is used, not taking into account the effect of damping on the eigenmodes.

Non-linearity cannot be included in the superelement matrices. However the superelements can be linked to other components with non-linear behaviour. E.g. it would be possible to consider friction in the VVGS, by using standard non-linear elements and connecting them to the superelements presented in this paper.

3. Validation of the simplified model

The mass and CoG of the simplified and benchmark models have been extracted, considering the reaction forces and the moments. The results have given a perfect match between the two models.

In order to verify the validity of the methodology used to obtain the simplified model, the following verification analyses were performed:

- Modal analysis;
- Power Spectral Density (PSD) analysis.

3.1. Modal analysis

For the modal analyses, constraints have been applied at the bottom of the VVGSs. The Block Lanczos modal solver has been selected in order to extract all the significant modes between 0 and 34 Hz.

The response of the simplified model is compared to that of the benchmark model. The main modes of the structure are reproduced with excellent fidelity. Fig. 10 shows the cumulative mass fraction comparison.

Table 1 lists the frequency and the effective mass of the main modes of the simplified model of the VV, while Table 2 lists the discrepancy with respect to the equivalent values obtained from the benchmark model.

Figs. 11 and 12 show examples of comparisons of modal shapes between simplified and benchmark models.

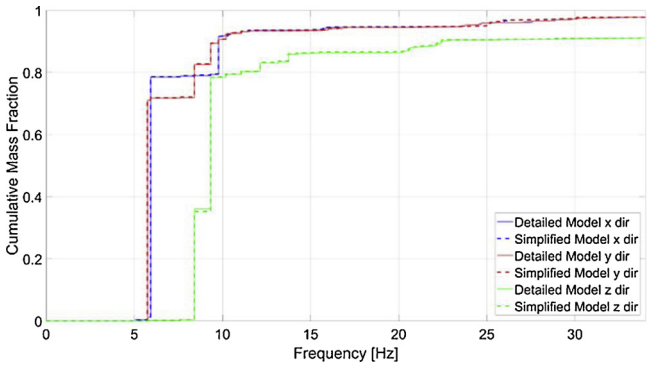

Fig. 10. Cumulative mass fraction for benchmark (Detailed) and simplified model of the VV.

Table 1
Frequency and effective mass of the main modes of the simplified model of the VV.

Mode #	Frequency [Hz]	Effective mass [tons]		
		X	Y	Z
2	5.7372	70	6001	20
3	5.9209	6537	62	1
5	8.4006	14	904	2945
6	9.3370	33	560	3647
7	9.7734	1024	111	9

Table 2
Discrepancy from the benchmark model. The error is normalized to the total mass of the VV.

Mode #	Frequency [%]	Effective mass [%]		
		X	Y	Z
2	−0.25	0.09	0.05	−0.01
3	−0.23	0.08	0.08	0.00
5	−0.18	0.00	0.10	0.86
6	−0.02	0.00	−0.21	0.98
7	−0.05	−0.17	0.06	0.03

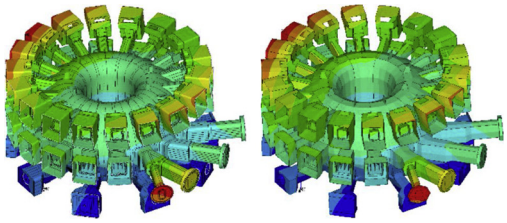

Fig. 11. Mode #3 – 5.29 Hz – X main mode: benchmark model (left) and simplified model (right).

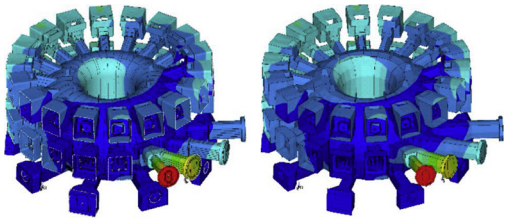

Fig. 12. Mode #6 – 9.33 Hz – Z main mode: benchmark model (left) and simplified model (right).

Table 3
Modal analysis computational time comparison.

Model	Time [s]
Detailed model	25000
Simplified model	240

Using the simplified model the computational time is reduced by approximately of 2 orders of magnitude. Table 3 lists the computational time comparison between detailed benchmark and simplified models.

3.1.1. Modal assurance criterion (MAC)

The MAC is a widely used tool for quantitative comparison of modal vectors. It is a statistical indicator, i.e. a coherence function [10], [11]. In the present study, the MAC is applied to compare the mode shapes of the benchmark model with those of the simplified model.

For each modal vector, the MAC takes a value equal to zero, if there is no consistent correspondence between the two modal vectors from the two models, to one, if there is full consistent correspondence. If the simplified model perfectly replicates the modes of the detailed one, the MAC plot would:

- Have a square base, as the number of modes in both models would be identical.
- Have a diagonal of red lines, indicating perfect correspondence between equivalent modes.
- Have mostly blue lines for the out-of-diagonal terms.

Fig. 13 shows the MAC comparison between the benchmark and the simplified models. Although there are a good number of red lines in the diagonal, there are places where the diagonal does not have a MAC close to one. In addition, there are more modes with frequency lower than 34 Hz in the detailed model than in the simplified one.

The reason for the 'gaps' in the diagonal is the large number of identical port extensions. As each extension has local modes with almost identical natural frequencies, all port modes have shapes that involve movements of several ports at once. In both models the number of modes associated with such local deformation is identical, and the frequencies match well. However, the two models tend to have different combinations of ports that are excited in any given mode. This means that the correspondence between these port modes is poor.

The benchmark model has more modes than the simplified model due to the fact that the simplified model has deliberately been built to not capture modes of the divertor cassettes. Modes from local motion of the divertors in the benchmark model therefore have no equivalents in the simplified model.

3.2. PSD analysis

In order to determine whether or not the simplified model is suitable despite the lack of a perfect diagonal in the MAC, further verification has been performed using PSD analysis. A wide input spectrum has been used, with a PGA of 0.315 g, applied at the bottom of the VVGS.

When response spectra extracted at various locations inside the benchmark and simplified models are compared, it is clear that the differences are very small. Where noticeable differences exist they are at high frequencies, and in regions highly affected by the local motion of the structure (e.g. Equatorial port connecting ducts, Lower port extensions, etc.).

Fig. 14 shows a comparison of a typical set of spectra. As can be seen, the correlation is very good. Fig. 15 represents the location where the discrepancy between benchmark and simplified model is the highest out of 369 locations that have been checked. Even here, the correlation is still acceptable considering that due to the dynamic characteristics of

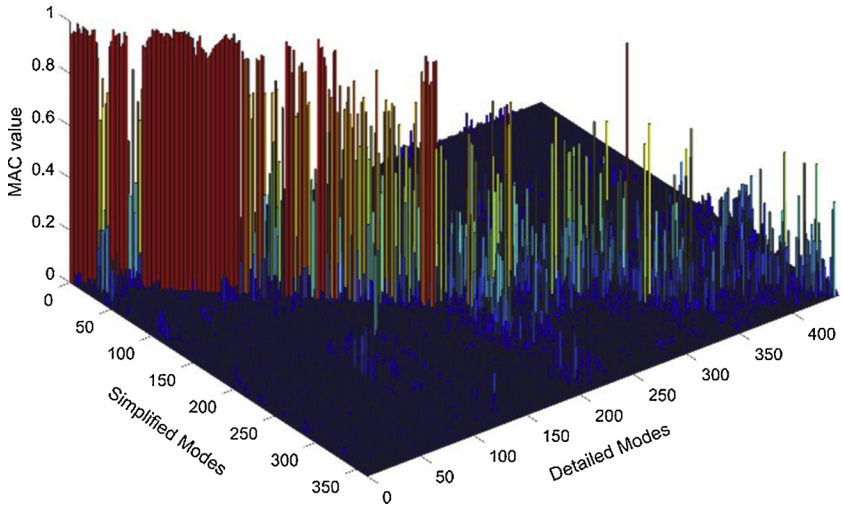

Fig. 13. 3D view of the MAC comparison of benchmark and simplified models of the VV.

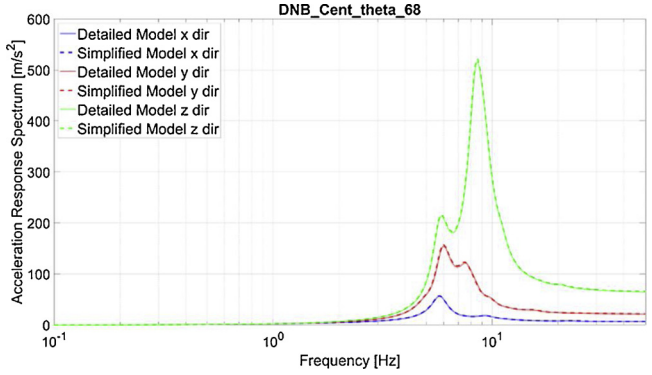

Fig. 14. FRS comparison – DNB flange centre point.

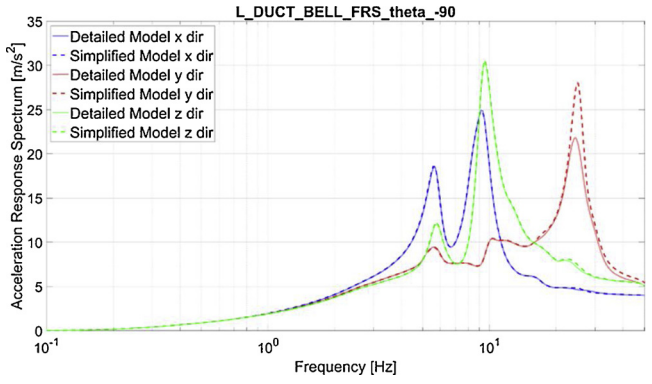

Fig. 15. FRS comparison – End of the lower port extension.

the Tokamak Complex there is little input energy above 20 Hz. Thus, although the model is less accurate above this frequency, it has little practical impact on the behaviour of the complete system during an earthquake. It would be possible to increase the fidelity of the results by increasing the number of nodes considered in the substructuring phase.

4. Conclusions

In the present study the substructuring methods has been shown to allow the creation of suitable simplified models. This method reproduces well the modal behaviour of the benchmark model, reducing the computational time to perform modal analyses by approximately two orders of magnitude.

In terms of the main modes of the structure, it has been shown that the maximum discrepancy between simplified and benchmark model frequency is 0.25%, with consistent mass contribution.

Using a combination of MAC and PSD analysis, it has been demonstrated that the generated simplified model behaves very similarly to the detailed model, and is therefore suitable for use in global seismic analyses. In terms of the spectra, errors of the order of 20% can be found, but at frequency values which are not expected to be excited, and have small impacts on the final results.

Considering the results achieved and presented in this paper it can be claimed that the technique used is suitable for the generation of simplified models of complex structures intended for global seismic analyses.

Disclaimer

The views and opinions expressed herein do not necessarily reflect those of the ITER Organization.

Declaration of Competing Interest

The authors declare that they have no known competing financial interests or personal relationships that could have appeared to influence the work reported in this paper.

References

[1] F. Di Martino, et al., Simplified models of the ITER vacuum vessel for global seismic analyses, Fusion Eng. Des. 136 (2018) 1354–1358.
[2] B. Besselink, et al., A comparison of model reduction techniques from structural dynamics, numerical mathematics and system and control, J. Sound Vib. 332 (2013) 4403–4422 2013.
[3] G.I. Schueller, Model reduction and uncertainties, in: structural dynamics, M. Papadrakakis, G. Stefanou, V. Papadopoulos (Eds.), Computational Methods in Stochastic Dynamics, Springer, 2011, pp. 1–24 Ch. 1.
[4] R. Guyan, Reduction of stiffness and mass matrices, AIAA Journal, American Institute of Aeronautics and Astronautics 3 (2) (1965) 380.
[5] D. de Klerk, et al., General framework for dynamic substructuring: history, review and classification of techniques, Aiaa J. 46 (May 5) (2008).
[6] N. Bouhaddi, R. Fillod, A method for selecting master DOF in dynamic substructuring using the Guyan condensation method, Comput. Struct. 45 (S/6) (1992) 941–946.
[7] ANSYS Mechanical APDL Theory Reference, Release 17.0, January, ANSYS Inc., 2016.
[8] https://www.sharcnet.ca/Software/Ansys/17.0/en-us/help/ans_cmd/Hlp_C_RBE3.html.
[9] Regulatory Guide 1.61 – Damping Values for Seismic Design of Nuclear Power Plants, U.S. Nuclear Regulatory Commission, Washington DC, 2007 20555-0001, March.
[10] M. Pastor, et al., Modal assurance criterion, Procedia Eng. 48 (2012) 543–548.
[11] L. Li, et al., Direct way of computing the variability of modal assurance criteria, Mech. Res. Commun. 55 (January) (2014) 53–58.